

Carbon-supported platinum and nickel nanoparticles for CO capture in hydrogen fuel cells

D. J. D. Durbin^{*}, D. Plana^{**}, D. J. Fermin^{**}, C. Malardier-Jugroot^{*}

^{*}Department of Chemistry and Chemical Engineering, Royal Military College of Canada
Kingston, Ontario K7K 7B4, cecile.malardier-jugroot@rmc.ca

^{**}School of Chemistry, University of Bristol
Bristol BS8 1TS, UK, david.fermin@bristol.ac.uk

ABSTRACT

Hydrogen fuel cells (HFCs) are increasingly looked at as an important and promising source of clean energy with the potential to replace internal combustion engines in automobiles. However, current HFC use is limited by carbon monoxide poisoning of the anode catalyst. Therefore, the present project investigates membranes of metal nanoparticles decorated on sp^2 -hybridized carbon surfaces that can be placed outside a fuel cell to capture CO before it enters the cell and poisons the anode catalyst. Density functional theory studies were performed with several metals on a small sp^2 -hybridized carbon surface. It was found that CO adsorbs most strongly to platinum, followed closely by nickel. These results were investigated electrochemically for platinum and nickel nanoparticles decorated on several carbon substrates. It was found that CO adsorbs more strongly to Pt than Ni in all systems. However, the strength of CO adsorption to Pt is affected by the type of carbon substrate.

Keywords: hydrogen fuel cells, carbon monoxide, anode poisoning, metal nanoparticles, sp^2 -hybridized carbon

1 INTRODUCTION

Hydrogen fuel cells (HFCs) are electrochemical cells that generate energy from the oxidation of hydrogen at the anode and reduction of oxygen at the cathode to produce H_2O . They have been given a lot of attention recently due to the growing need for high efficiency energy conversion technologies. HFCs are especially important because they have the potential to replace internal combustion engines in automobiles [1].

At present, hydrogen gas is produced by reforming hydrocarbons, which produces CO and CO_2 as by-products. Carbon dioxide has little effect on the fuel cell. However, when CO enters the cell, it adsorbs irreversibly to the platinum anode catalyst, preventing H_2 binding and oxidation. Many CO-tolerant catalysts have been investigated with notable success. However, the ideal solution is still to remove CO from the H_2 feed gas before it enters the cell [2].

The present work focuses on the development of an sp^2 -hybridized carbon membrane decorated with metal nanoparticles. It will be placed external to the fuel cell to

capture CO before it enters the cell. The membranes would be removed and regenerated by removing CO as needed. The presence of such a membrane would greatly increase cell efficiency, in addition to reducing production costs if produced with non-precious metals.

Density functional theory (DFT) studies examined sections of sp^2 -hybridized carbon decorated with different transition metals. Undoped carbon surfaces were investigated, as well as those containing boron, oxygen or nitrogen substitutional dopants. The durability of the metal particles on the carbon surfaces and the strength of CO and H_2 binding were calculated. An ideal surface should have strong metal/C binding, as well as strong binding to CO and weak interaction to H_2 [3,4].

DFT was used because it is a powerful modeling tool. It is especially useful for large systems because it computes quantum information using electron density instead of Schrödinger's wave equation; this drastically decreases computation time [5]. In addition, DFT has proven effective for modeling similar systems [6].

Theoretical studies found that platinum and nickel are the most promising metals for CO-capture membranes. Therefore, Pt/C and Ni/C systems were investigated electrochemically in aqueous solution to confirm theoretical results and determine the effect of the carbon substrate on the metal's catalytic properties.

CO stripping voltammetry was used as a tool to observe trends in CO binding to Pt and Ni on various carbons. This was used as a first approximation to confirm the trends obtained by DFT calculations. Additionally, the electrochemical experiments provide information on the behaviour of CO in a fuel cell with a carbon-supported catalyst.

Electrochemical measurements are often used for analysis of CO adsorption on transition metals, especially Pt, because CO is an ideal model compound due to being the smallest C_1 molecule that can be oxidized in low temperature fuel cells. In addition, other C_1 molecules, such as methanol and formic acid, produce CO as an intermediate during oxidation [7].

2 THEORETICAL STUDIES

All simulations were performed using density function theory (DFT) with the B3LYP functional and the

LANL2MB basis set using *Gaussian 03* software package [8] on a Mac OS X Leopard 10.6.2 system. This combination of functional and basis set has been previously shown to produce accurate results for comparable systems [6].

The graphene surface was constructed of fourteen graphene rings with terminal hydrogen atoms. For doped surfaces, one dopant (boron, nitrogen, oxygen) atom replaced one carbon atom in the centre of the graphene surface. Each doped graphene system was geometrically optimized before one metal atom was placed above the surface and the entire system re-optimized (fig. 1). The systems were analyzed separately with CO and H₂ gas. The binding energy of the metal to the graphene surface was then measured in the absence and presence of feed gas molecules (equations E1 and E2 respectively). Finally, the binding energy of each feed gas component to the metal/graphene system was calculated by equation E3.

$$BE_{\text{metal-graphene}} = E_{\text{metal-graphene}} - E_{\text{graphene}} - E_{\text{metal}} \quad (\text{E1})$$

$$BE_{\text{metal-graphene}} = E_{\text{metal-graphene-gas}} - E_{\text{graphene}} - E_{\text{metal-gas}} \quad (\text{E2})$$

$$BE_{\text{metal-graphene-gas}} = E_{\text{metal-graphene-gas}} - E_{\text{metal-graphene}} \quad (\text{E3})$$

DFT studies analyzed the durability of the metal particles on a graphene layer (defined here as metal-graphene binding energy) for each system. It was found that platinum has a stronger interaction with graphene than nickel. In both systems the addition of dopants increases metal-graphene binding; oxygen has the largest effect. CO and H₂ binding on both systems was also calculated. It was found that CO has the strongest binding to carbon-supported platinum followed closely by nickel (BE_{Pt-CO} = 350.79 kJ, BE_{Ni-CO} 324.80 kJ). Of these metals, nickel has a notably weaker interaction with H₂ (BE_{Pt-H₂} = 144.61 kJ, BE_{Ni-H₂} = 54.40 kJ). Addition of boron, nitrogen or oxygen dopants to the carbon surface decreases CO binding by up to 17% for Pt and 28% for Ni. Addition of dopants also causes H₂ binding to become negligible on all systems.

3 EXPERIMENTAL

3.1 Materials and reagents

Chloroplatinic acid solution (8 wt% in H₂O) (262587), graphite (1-2 μm diameter, synthetic) (282863), Nafion perfluorinated ion-exchange resin (10 wt% in H₂O) (527106) and single-walled carbon nanotubes (carbon >90 %, ≥70% carbon as SWCNT, 0.7-1.3 nm diameter) (704113) were purchased from Sigma-Aldrich. Nickel chloride hexahydrate (12372) was purchased from Alfa Aesar. Carbon nanocoils were synthesized by Dr. Lázaro and co-workers at the Instituto de Carboquímica in Spain [9]. Ultra-pure water obtained from a Millipore MilliQ system was used for all reactions. All other solvents and reagents were standard laboratory grade.

3.2 Metal/carbon synthesis

3.2.1 Platinum decoration. The desired carbon substrate (80 mg) was added to water at a concentration of 1 g/L. It was then dispersed by sonication, followed by stirring for 1 hour each. The dispersion was then placed back into the sonicator. While in the sonicator, chloroplatinic acid (525 μL) dissolved in 35 mL water (clear, bright yellow solution) was added at the rate of 1 mL every 5 min. The physical appearance of the carbon substrate (black powder) did not change, but the yellow colour of the H₂PtCl₆ solution disappeared upon addition to the carbon substrate. After addition of the H₂PtCl₆ solution was complete, the Pt^{II}/C dispersion was sonicated for an additional 20 minutes. The pH was adjusted to 5 with 0.1 M NaOH solution. The dispersion is then stirred overnight.

The following day, a solution of NaBH₄ (20 mL, 1 g/L) was added to the Pt^{II}/C dispersion at a rate of 1 mL every 3 min in a sonicator maintained at 5-6 °C. Following the addition of the NaBH₄ solution, the Pt⁰/C dispersion was left in the sonicator for an additional hour. The dispersion was then stirred overnight. The next day, the Pt/C dispersion was vacuum filtered; the black precipitate was collected and dried in an oven at 60-70 °C overnight [10].

3.2.2 Nickel decoration. The desired carbon substrate (40 mg), nickel chloride hexahydrate (24 mg, light green powder) and ethylene glycol (40 mL) were placed in a Schlenk flask under nitrogen. This produced a dispersion of black precipitate in a clear, colourless solution. The mixture was stirred for 4 hours to allow the nickel (II) to interact with the carbon substrate. After 4 hours, the solution was degassed by bubbling N₂ through the solution for 10 min. The flask was then opened back to nitrogen and hydrazine hydrate (95 μL) was added to the solution, followed by sodium hydroxide (0.4 mL of 1M solution). The reaction was then stirred in an oil bath heated at 65-70 °C for one hour. After this time, the reaction was stopped and the black precipitate isolated by vacuum filtering. The sample was then washed with H₂O followed by ethanol and dried in a Schlenk tube (ca. 10⁻² mbar) overnight [11].

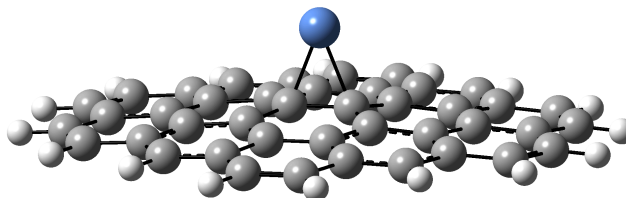


Figure 1 – Simulated 14-ring graphene surface containing a nickel atom (blue=nickel, grey=carbon, white=hydrogen).

3.3 Electrochemical measurements

Electrochemical experiments were performed using a MicroAutolab potentiostat connected to a three-electrode

cell containing a platinum counter electrode and an Ag/AgCl reference electrode contained within a Luggin capillary. The working electrode was prepared by allowing a metal/C ink (20 μL) to dry on a glassy carbon surface. The ink was prepared by dispersing the metal/C sample (3 mg) with Nafion (15 μL) in water (500 μL). The cell was filled with sulphuric acid solution (0.5 M), which was deaerated by argon gas for ca. 30 min.

The electrochemically active catalytic area was measured from CO-stripping voltammograms by integration of the CO_{ad} oxidation region, assuming a charge of 420 $\mu\text{C}/\text{cm}^2$ for a monolayer coverage of linearly adsorbed CO. Carbon monoxide was adsorbed on the platinum surface by bubbling CO through the solution for 10 min at -0.166 V. The solution was then purged with argon for ca. 20 min to remove excess CO from the solution before the CO-stripping voltammogram was acquired.

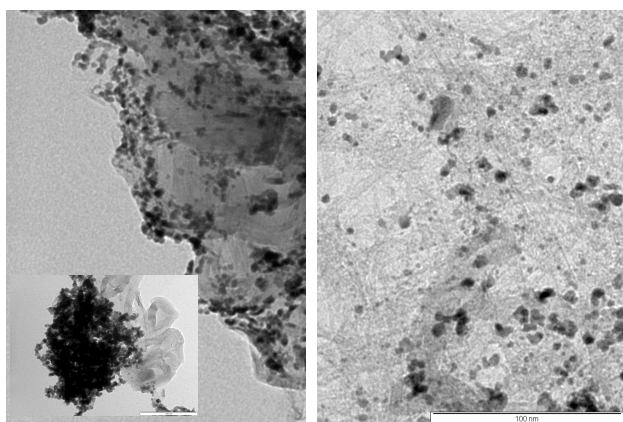


Figure 2 – Platinum-decorated carbon nanocoils (left) and single-walled carbon nanotubes (right). The insert shows a platinum aggregate beside undecorated CNCs. Scale bar is the same for both full sized images; it represents 100 nm.

3.4 Characterization

Transmission electron microscopy (TEM) images were acquired on a JEOL JEM 1200 EX Mk 2 microscope with a standard tungsten filament operated at 120KV with magnifications up to 1 million. Images were recorded with a MegaView III digital camera using Soft Imaging Systems GmbH analySIS 3.0 image analysis software.

TEM samples were prepared by adding a small amount of sample to pure ethanol in a small vial. The sample was then sonicated for ca. 5 min to separate any aggregates. It was then dropped onto a pre-carbon coated copper TEM grid and allowed to air dry.

X-ray diffraction (XRD) patterns were obtained using a Bruker AXS D8 advance diffractometer with $\text{CuK}(\alpha)$ radiation and a θ - θ configuration.

BET measurements were performed on a Quantachrome Autosorb-1 using Autosorb Data Acquisition Software Micropore (version 2.10) to acquire nitrogen isotherms containing 39 data points.

4 RESULTS AND DISCUSSION

Platinum and nickel were deposited on single-walled carbon nanotubes (SWCNT), carbon nanocoils (CNC) and graphite powder. These carbon substrates were chosen because they are composed primarily of sp^2 -hybridized carbon, but each substrate has a unique structure with a high surface area. SWCNTs and CNCs are nanomaterials, while graphite is several orders of magnitude larger (in the micron scale). It is expected that metal-decorated nanostructured carbon materials will show better catalytic properties.

4.1 Carbon substrate

TEM images show that metal nanoparticles adhere evenly to SWCNTs (fig. 2 right). In contrast, on CNCs (fig. 2 left), some metal nanoparticles adhere to the carbon substrate while others form metal aggregates. Analysis of XRD spectra show the area of the metal nanoparticles to be 28 nm^2 on CNCs and 25 nm^2 on SWCNTs. This is consistent with the nanoparticle areas calculated from analysis of TEM images.

Adsorption-desorption isotherms (not shown) show typical H_4 hysteresis for SWCNTs, which suggests the presence of slit-shaped micropores. This does not change when Pt is added to the system. In contrast, the hysteresis in CNC systems extends through the full range of measured pressures. This suggests the presence of intercalated gas molecules. Therefore, the N_2 molecules likely become trapped within the nanocoil structure. As a result, they do not desorb even at very low pressures. This effect is observed both in the presence and absence of Pt [12,13].

BJH desorption plots indicate the presence of micro and mesopores in SWCNTs with diameters ranging from 15 to 50 \AA . Carbon nanocoils show only mesopores with a diameter of approximately 40 \AA . The amount of micropores increases for both systems when Pt nanoparticles are added.

4.2 CO-stripping

CO-stripping voltammograms of platinum-decorated SWCNTs, CNCs and graphite (fig. 3, Table 1) show strong binding of CO to platinum nanoparticles in all systems. However, there are many differences observed between the two voltammograms. First, CO desorption occurs at a more positive potential ($\Delta E = 0.07\text{V}$) for platinum on SWCNTs than the other carbon substrates. This suggests that CO binds more strongly to Pt in this system. Second, the Pt/CNC system shows two CO desorption peaks while voltammograms for the other systems show only one. This suggests a distribution of Pt-CO binding energies that likely results from the presence of low coordinated Pt. Since XRD analysis suggests that the platinum nanoparticles are very similar in both SWCNT and CNC systems, this difference

is likely a result of the carbon substrate. The discrepancy could originate because SWCNTs are more finely organized structures than CNCs.

In CO-stripping voltammograms for nickel systems (not shown), the CO-desorption peak (Table 1) occurs at a more negative potential ($\Delta E = 0.14\text{-}0.24\text{V}$). This suggests that CO is removed from Ni much more easily than Pt. This is in agreement with DFT calculations [3]. Electrochemical results also suggest that Ni-CO binding is less affected by the type of carbon substrate than Pt-CO binding.

Table 1: CO desorption peak potential onset and apex for CO-stripping voltammograms of Pt-decorated SWCNTs, CNCs and graphite and Ni-decorated SWCNTs and CNCs

Metal	Substrate	Peak onset (V vs. Ag/AgCl)	Peak apex (V vs. Ag/AgCl)
Pt	SWCNT	0.37	0.55
	CNC	0.38	0.48
	Graphite	0.35	0.48
Ni	SWCNT	0.24	0.34
	CNC	0.23	0.31

5 CONCLUSION

Metal-decorated sp^2 -hybridized carbon substrates have great potential use as CO-capture membranes in hydrogen fuel cells. Electrochemical measurements in aqueous solution show that CO binds more strongly to Pt-decorated carbon substrates than Ni-decorated substrates. The effectiveness of metal nanoparticles to bind CO depends on the morphology of the carbon substrate, especially in Pt systems. Single-walled carbon nanotubes produce the strongest CO adsorption to metal nanoparticles. Therefore, they are ideal for CO-capture membranes. Conversely, SWCNTs should not be used as the carbon support for metal catalysts in hydrogen fuel cells because they will be easily poisoned by any CO remaining in the feed gas.

6 ACKNOWLEDGEMENTS

The authors thank Verónica Celorrio Remartinez for providing carbon nanocoils; George Dowson, Dr Judy Hart, Dr. Avinash Patil and Dr. Laurent Chabanne for assistance with synthetic procedures; Dr. Keith Bean and Martha Thompson for assistance with analytical techniques; Dr. Thomas Davies for use of specialize equipment; Jonathan Jones from the Electron Microscopy Unit at the University of Bristol for TEM services; and Dr. Stuart Prescott and Prof. Terence Cosgrove for advice and support.

Funding and resources for this project were provided by Natural Sciences and Engineering Research Council of Canada (NSERC), Defense and Security Research Institute and Royal Military College Defense Academic Research (DSRI – RMC DAR) Programme, Royal Military College of Canada and University of Bristol, UK.

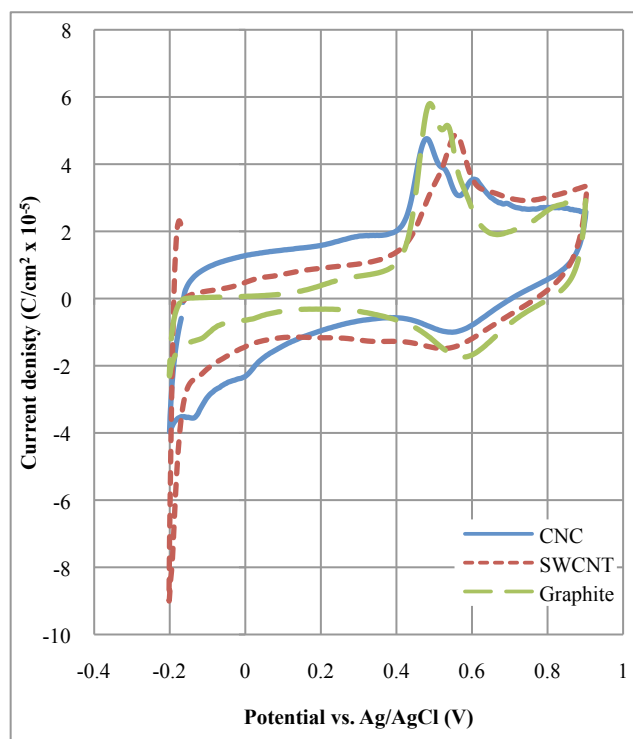


Figure 3 – CO-stripping voltammograms of Pt-decorated SWCNTs, CNCs and graphite in deaerated 0.5 M H_2SO_4 with $v = 20\text{mV s}^{-1}$.

REFERENCES

- [1] Carrette, L., et. al. (2000) *Chem. Phys. Chem.* 1, 162-193
- [2] Gamara, G. A., et al. (2002) *J. Electrochem. Soc.* 149: A748-A753
- [3] Durbin, D. J. D., Malardier-Jugroot, C. (2011) *J. Phys. Chem. C* 115, 808-815
- [4] Durbin, D. J. D., Malardier-Jugroot, C. *J. Phys. Chem. C*. Submitted (March 2011)
- [5] Parr, R. G., Yang, W. (1989) *Density-Functional Theory of Atoms and Molecules*. Oxford Science Publications, New York, NY.
- [6] Groves, M, N., et al. (2009) *Chem. Phys. Lett.*, 481, 214-219
- [7] Marković, N. M., Ross, P. N., Jr. (2002) *Surf. Sci. Reports*, 45, 117-229
- [8] Frisch, M. J. (2004) *Gaussian 03*, Gaussian, Inc. Wallingford, CT
- [9] Celorrio, V., et. al. (2010) *Energy Fuels*, 24, 3361–3365
- [10] Lázaro, M. J., et al. *J. Power Sources*. Accepted.
- [11] Wu, S-H., Chen, D-H. (2003) *J. Colloid Interface Sci.* 259, 282–286
- [12] Barrer, R. M., MacLeod, D. M. (1954) *Trans. Faraday Soc.* 50, 980-989
- [13] Rouquerol, F., et. al. (1999) *Adsorption by Powders & Porous Solids*, Academic Press, London, 191-285